Tunable nanowire nonlinear optical probe

Yuri Nakayama[1,6]*, Peter J. Pauzauskie[1,5]*, Aleksandra Radenovic[2,4]*, Robert M. Onorato[1]*, Richard J. Saykally[1], Jan Liphardt[2,3,4], and Peidong Yang[1,5]

[1]Department of Chemistry, [2]Department of Physics, and [3]Biophysics Graduate Group, University of California, Berkeley, CA 94720, USA

[4]Physical Biosciences Division and [5]Materials Science Division, Lawrence Berkeley National Laboratory, Berkeley, CA 94720, USA

[6]Materials Laboratories, Sony Corporation, 4-16-1 Okata, Atsugi-shi, Kanagawa 243-0021, Japan

*These authors contributed equally to this work.

CONVERSION EFFICIENCY

Subwavelength nanowire cavities have been demonstrated to align spontaneously with the optical axis of the trap (*1*), automatically maximizing the overlap between the nanowire and trapping laser. This eliminates the need for mechanical components for the manual alignment of the subwavelength cavity. The need to enhance phase matching through techniques such as periodic poling of the crystal structure is not a concern for 2-photon conversion in this work since the normal nanowire lengths (Fig. S1a) are within a few coherence lengths, $L_c = \pi/|\Delta k| \sim 3$ μm, where Δk is the well-known phase matching term calculated by $|2\mathbf{k}_\omega - \mathbf{k}_{2\omega}|$. We assume a diffraction-limited spot for the optical trap due to the high numerical aperture (NA~1.2) of the water-immersion objective. Consequently, the nanowire's cross-sectional area is ~26% (calculated for typical nanowires shown in **Fig S1a**) of the diffraction-limited waist area. Thus, we use the short length and small cross-sectional area of the nanowire to select an infinite, non-depleted plane wave approximation (*2, 3*) for simulation of the

conversion efficiency for second harmonic generation. The maximum conversion efficiency, $\eta^{o}_{2\omega}$, is given by the expression:

$$\eta^{0}_{2\omega} = \frac{8\pi^2 \cdot d_{eff}^2 \cdot L^2 \cdot I_\omega}{\varepsilon_0 \cdot n_\omega^2 \cdot n_{2\omega}^2 \cdot c \cdot \lambda_\omega^2} \qquad \textbf{(0.1)}$$

where "d_{eff}" is the maximum effective nonlinear $\chi^{(2)}$ tensor element (~27 pm/V), "L" is the nanowire's length typically 5.4 μm, "I_ω" is the incident pump intensity (~1 W/μm^2), "n_ω" is the index of refraction in the [011] growth direction (n_ω=2.1 (*4*)) "*c*" is the speed of light, and "λ_ω" is the wavelength at the frequency ω. Using a "d_{eff}" value of 27 pV/m (*5*) the maximum possible conversion quantum efficiency would be 0.00014.

The overall conversion efficiency, $\eta_{2\omega}$, is determined by phase matching within the cavity and is calculated with the expression:

$$\eta_{2\varpi} = \eta^{0}_{2\omega} \frac{\sin^2\left(\frac{\Delta kL}{2}\right)}{\left(\frac{\Delta kL}{2}\right)^2} \qquad \textbf{(0.2)}$$

where Δk and "L" are defined as above. Consequently, the power of the beam at frequency I_{SH} 2ω generated in SHG scales with (*6*)

$$I_{SH} \propto I_F^2 \cdot L^2 \cdot (\chi^{(2)})^2 \cdot \frac{\sin^2\left(\frac{\Delta kL}{2}\right)}{\left(\frac{\Delta kL}{2}\right)^2} \quad \textbf{(0.3)}$$

Here I_F and I_{SH} are the power of the beams at ω and 2ω and $\chi^{(2)}$ is the nonlinear susceptibility of the nanowire.

We measured the SHG conversion efficiency of the trapped nanowire shown on **Fig S1a**. We varied the pump laser power and measured SHG signal using an Andor iXon DV 877 front illuminated CCD camera with single photon detection capability. We took great care to filter out any accompanying pump-laser light (1064 nm) by using a filter set consisting of a holographic filter (super notch >10^{-6} Opticsland) and two IR cut-off filters (XF-86 Omega Optical). In addition to the IR filters we also used a 532 nm band pass optical element (FB530-10 Thorlabs).

Using a previously developed method (*1*) we were able to attach $KNbO_3$ nanowires to the top coverslip and later measure geometrical characteristics with an atomic force microscope AFM. From AFM measurements we obtained precise information on the nanowire's width, height, and length. We were able to calculate, with this information, the maximum theoretical conversion efficiency using expression above. The data are shown in **Fig. S1c**. Our experimental results are shown in red; overall they are ~2 times smaller than the maximum theoretical conversion efficiency.

RESOLUTION

Using a previously reported method[1], lateral displacements of the nanowire due to the nanowire Brownian motion at typical trapping powers are calculated to be on the order of 10 nm with typical frequency of ~100 Hz **Fig S1d**. Thus, the lateral fluctuation time is 10^{10} times longer than the time it takes a 532 nm photon to travel the length of the nanowire (~74 fs for a 10 μm long wire). As a result, lateral thermal wire fluctuations are not likely to affect frequency doubling in the optical potential.

The high speed CCD was used to record time-dependent SHG signal from optically-trapped nanowires. There were minimal fluctuations on 100s time-scales with root-mean-square deviations from the mean less than 0.2% (**Figure S3a**).

Potential azimuthal rotation of the wire about its growth axis makes it difficult to specify a particular effective nonlinear susceptibility (d_{eff}) value for use in calculations.

Waveguiding of the generated second-harmonic is strong given the high index of refraction in the [011] growth direction (n = 2.21 (*4*)). The calculated evanescent 1/e decay distance of 532 nm light from the $KNbO_3$ cavity wall is calculated to be ~50 nm in liquid water.

Synthetic challenges remain in that the nonlinear $\chi^{(2)}$ tensor elements depend heavily on the nanowire's growth direction within $KNbO_3$'s anisotropic perovskite crystal structure. We used the wire in an analogous way to the scanning near-field optical (NSOM) excitation configuration.

There are many factors which influence the contrast and resolution during NSOM imaging such as tip-sample separation, collection optics, polarization of the illumination and most importantly aperture size. In 1984 Pohl et al (*7*) demonstrated a

near-field optical imaging system based on metal-coated etched quartz tips to form the aperture. Betzig and Trautman (*8*) made a major improvement on Pohl et al's scheme by tapering the optical fiber to form probe. The tapering was done by mechanically pulling the fiber while locally heating it with CO_2 laser. The aperture was formed by coating the pulled tip at an angle to avoid covering the end face. This technique increased the technique resolution.

We also demonstrate that resolution will be affected by the aperture size. **Figure S2** shows two line scans obtained with nanowires having different dimensions. For the thick wires (**Fig S2 a,b**) it wasn't possible to resolve all 9 gold lines deposited on the glass coverslip. The typical inverted SHG signal reveals only 8 peaks (**Fig S2 c**). In contrast, when a thin wire is used (**Fig S2 d,e**) all 9 gold structures are revealed (**Fig S2 f**). In addition, the mean thickness of the peaks is smaller than for the line scans taken with the thick $KNbO_3$ nanowires. However in the retrace we can resolve only 8 peaks most likely due to opto-mechanical deflections (**Fig S3 b-c**).

Improvements in synthesis of semiconductor nanowires provide hope that the synthesis of the $KNbO_3$ nanowires will mature and eventually yield thin, uniform $KNbO_3$ nanowires. Potassium niobate is an ideal material for this purpose due to its benign elemental composition (*9*).

ONE vs. TWO PHOTON FLUORESCENCE EXCITATION

We attempted to gain insight into the ability of nanowires to excite molecular fluorescence via comparison of nanowire-probe fluorescence excitation with conventional two-photon excitation (2PE) (**Fig. S4**). Two-photon luminescence must be considered for an accurate measurement of the nanowire probe's fluorescent signal. Two-photon fluorescence spectra (not shown) of a dilute solution of POPO-3 molecules were taken as described in the methods section. Due to the small two-photon absorption cross section ($\delta \sim 10^{-58}$ m^4/s) of the dye, extremely high photon fluxes ($\sim 10^{30}$ $cm^{-2}s^{-1}$) are required to enable sufficient probability for two-photon excitation.

Spectra were also taken while a $KNbO_3$ nanowire was optically trapped. The resulting spectra from simultaneous nanowire-SHG (NW-SHG) and 2PE, is plotted in (**Fig. S4**, red line). In order to differentiate respective contributions to fluorescence

spectra during simultaneous [NW-SHG, 2PE] excitation (red line), the baseline spectra from pure 2PE was subtracted from the composite spectra (blue line). The integrated spectral intensity for composite [NW-SHG, 2PE] excitation was approximately 2.2 times larger than the corresponding value for exclusive NW-SHG excitation. Consequently, the effective fluorescence intensity produced from single-photon excitation by the nanowire-probe is comparable to that of standard two-photon excitation. Presumably, this is possible because of the larger absorption cross-section for one-photon excitation (*10*). Exact comparison of NW-SHG and 2PE intensities is complicated by the back-scattering geometry used to collect fluorescence, in which the wire waveguides 532 nm photons away from the collection plane while simultaneously acting as a physical obstruction to collection of the excited fluorescence through the lower objective.

REFERENCES

1. P. J. Pauzauskie *et al.*, *Nature Materials* **5**, 97 (Feb, 2006).
2. R. L. M. Sutherland, D. G. Kirkpatrick, *Handbook of Nonlinear Optics*. 2nd, Ed. (Dekker, New York, 2003), pp.
3. R. L. M. Sutherland, D.G.;Kirkpatrick, S., *Handbook of Nonlinear Optics* (Dekker, New York, ed. 2nd., 2003), pp. 44.
4. *SNLO nonlinear optics code available from A.V. Smith, Sandia National Laboratories, Albuquerque NM 87185-1423*.
5. W. R. Cook, R. F. S. Hearmon, H. Jaffe, D. F. Nelson, *Numerical Data and Functional Relationships in Science and Technology*. N. Series, Ed. (Springer, Berlin, ed. Hellwege, K.H. Hellwege, A.M., 1979), pp.
6. Y. R. Shen, *The Principles of Nonlinear Optics* (Wiley, New York, 1984), pp.
7. D. W. Pohl, W. Denk, M. Lanz, *Applied Physics Letters* **44**, 651 (1984).
8. E. Betzig, J. K. Trautman, T. D. Harris, J. S. Weiner, R. L. Kostelak, *Science* **251**, 1468 (Mar 22, 1991).
9. Y. O. Atsuo Ito, Tetsuya Tateishi, Yoshimasa Ito, *Journal of Biomedical Materials Research* **29**, 893 (1995).
10. W. Denk, J. H. Strickler, W. W. Webb, *Science* **248**, 73 (Apr 6, 1990).

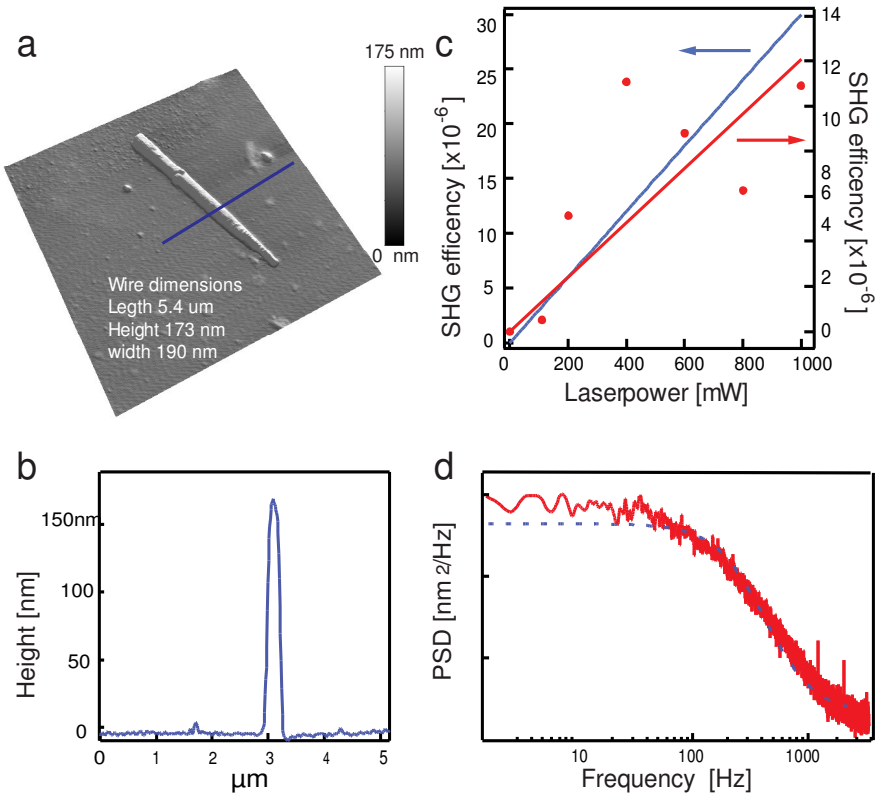

Figure S1. a AFM micrograph of $KNbO_3$ nanowire with corresponding line scan **b, c** theoretical (blue) and experimental (red) SHG conversion efficiencies as a function of laser power for the trapped $KNbO_3$ nanowire **d** power spectrum of PSD sum signal fluctuations for a $KNbO_3$ nanowire trapped at 400-mW power.

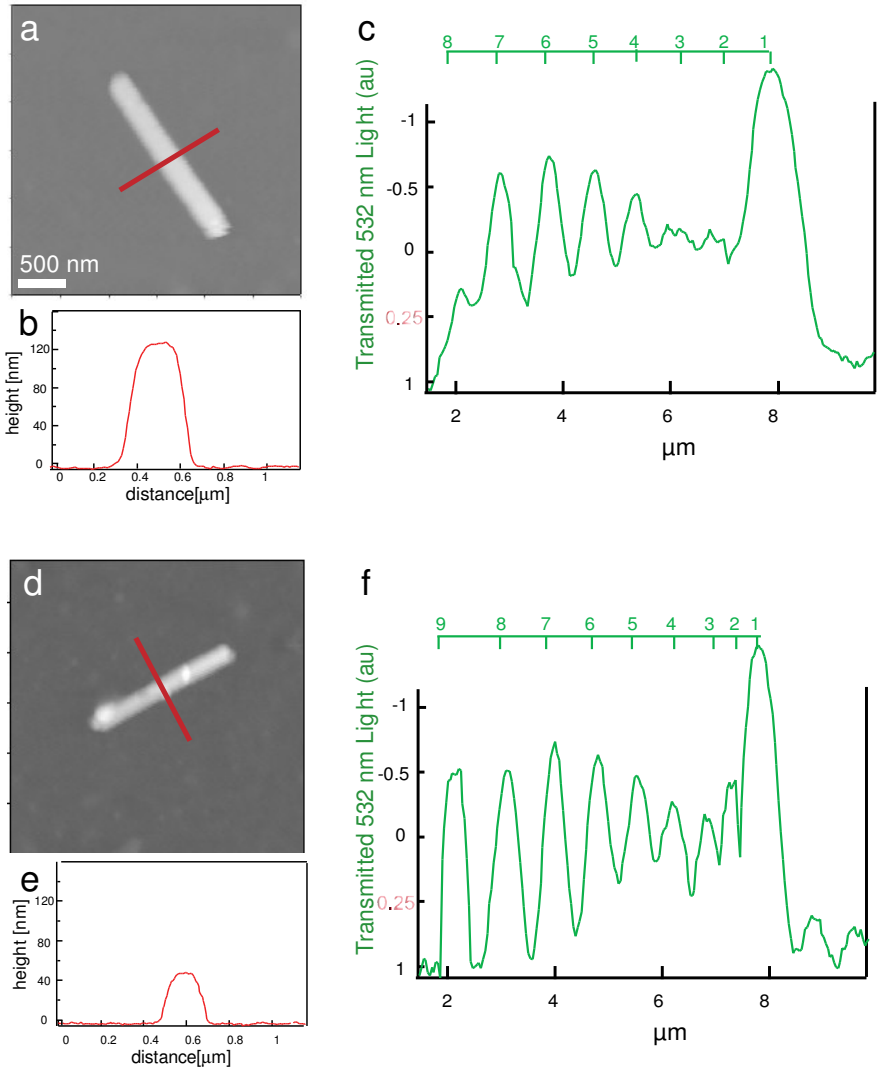

Figure S2. a AFM micrograph of thick $KNbO_3$ nanowire with corresponding AFM line scan **b** which reveals wire dimensions width=270nm, length =2μm and height=136 nm **c** line scan from the thick $KNbO_3$ nanowire SHG signal taken over the gold calibration pattern **d** AFM micrograph of the thin $KNbO_3$ nanowire with corresponding line scan **e** which reveals wire dimensions width=122 nm, length =1.4 μm and height=53 nm **f** line scan from the thin $KNbO_3$ nanowire SHG signal taken over the gold calibration pattern.

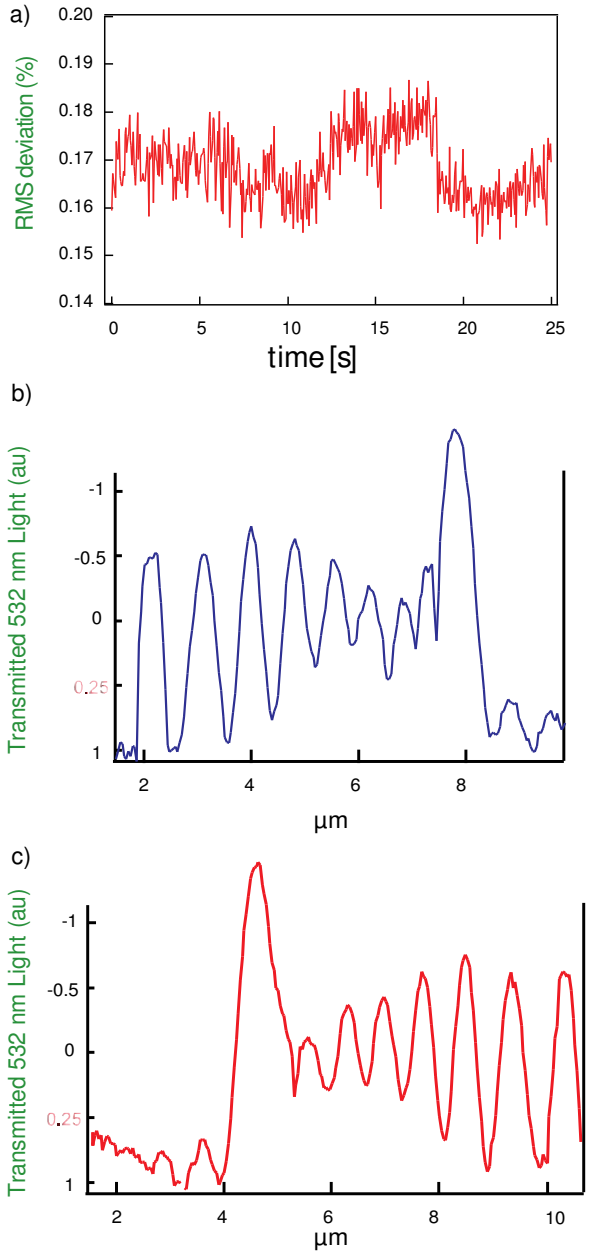

Figure S3. a Time trace for nanowire in figure S2d showing root mean square percentage from the mean. **b** trace and **c** retrace data for nanowire probe from **Fig. S2d**. Subtle changes in resolution occur due to drift of the top imaging objective.

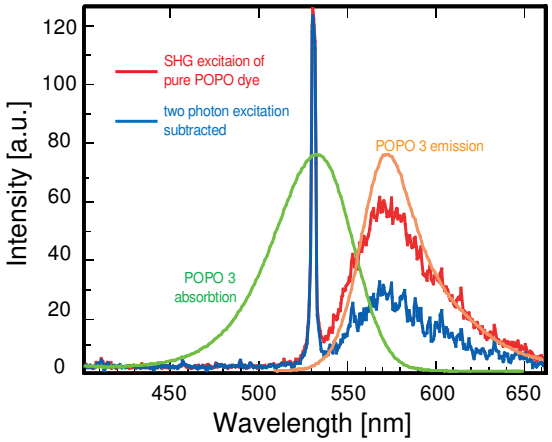

Figure S4. Spectral characteristics of POPO-3 and corresponding experimental data. Absorption (green) and emission (orange) data are plotted for POPO-3. The red trace shows the spectrum obtained from both SHG-excitation and two-photon excitation, while the blue trace shows the spectrum for SHG-excitation after subtraction of the two-photon contribution

Table S1: Comparison of pitch for gold lines measured by AFM and $KNbO_3$ nanoprobe optical transmission.

	Pitch	
Stripe	$KNbO_3$ (nm)	AFM (nm)
9	1112	1193
8	983	1071
7	898	974
6	812	876
5	727	754
4	684	657
3	598	535
2	470	414